Vol. 16, pp. 108–113 (2019)
doi: 10.2142/biophysico.16.0_108

Biophysics and Physicobiology
https://www.jstage.jst.go.jp/browse/biophysico/

Regular Article

Dynamic analysis of ribosome by a movie made from many three-dimensional electron-microscopy density maps

Atsushi Matsumoto

Molecular Simulation and Modeling Group, National Institutes for Quantum and Radiological Science and Technology, Kyoto 619-0215, Japan

Received February 8, 2019; accepted March 12, 2019

The atomic models of the 70S ribosome including the bound molecules were built from many 3D-EM density maps. The positions and conformations of the bound molecules were determined by fitting them to the regions in the density maps which remained after fitting the 70S ribosome. Then, using these atomic models, a movie for the elongation cycle was made. For determining the sequential order in which the models appeared in the movie, the knowledge about the bound molecules and the ratchet angles were used. The movie revealed several interesting points which were not apparent from each density map, suggesting the usefulness of a movie made from many 3D-EM density maps.

Key words: ratchet angle, elongation cycle, conformational change, 3D-EM, fitting

Determination of three-dimensional (3D) structures of macromolecules by the cryo-electron microscopy (cryo-EM) and the reconstruction techniques [1] is quite common these days. Although the resolution is usually lower than that in the X-ray crystallography, this method has an advantage in that the crystallization is unnecessary. Furthermore, the determined structures are expected to be close to those in solution or in a living organism.

It is also quite common to build an atomic model computationally from each 3D-EM density map, which is built from many EM images by the reconstruction techniques. The model-building usually consists of two steps [2–4]; one is the fitting of the X-ray crystal structure into the map and another is the deformation of the crystal structure to improve the fitting. Previously, we have developed an approach for the model-building from the EM density map [5]. In this approach, a library which consists of a huge number of atomic models with different conformations is built first by computationally deforming the X-ray crystal structure. Then, the best-fitting atomic model for each 3D-EM density map is selected from the library. Our approach is appropriate for the case in which many 3D-EM density maps of the same target are available, because the selection of the best-fitting model takes much less computational time than building the library.

Ribosome is a huge macromolecular complex responsible for protein synthesis. Because of its importance, many studies have been performed intensively. As of Feb. 2019, the Electron Microscopy Data Bank (EMDB) stores more than 250 3D-EM density maps of the prokaryote 70S ribosome. A different map usually corresponds to a structure in a different functional state of the ribosome. Thus, it might be possible to describe the entire life of ribosome by these 3D-EM maps.

The main purpose of this study is to reproduce the conformational changes of the 70S ribosome at the atomic

Corresponding author: Atsushi Matsumoto, Molecular Simulation and Modeling Group, National Institutes for Quantum and Radiological Science and Technology, 8-1-7 Umemidai, Kizugawa, Kyoto 619-0215, Japan.
e-mail: matsumoto.atsushi@qst.go.jp

◀ ***Significance*** ▶

Recent development of the cryo-electron microscopy enables structural analysis of a macromolecule in various functional states more easily than before. In this article, a movie of the 70S ribosome was made by combining multiple atomic models built from many EM density maps. The movie was found to be very useful for understanding the molecular mechanism.

resolution using many 3D-EM density maps. In this study, the elongation cycle was focused on, where an amino-acid is added to the growing polypeptide chain. The result is represented as a movie, and it will greatly promote our understanding about the molecular mechanism of the 70S ribosome.

Methods

Building atomic models for molecules bound to the 70S ribosome

We built the best-fitting atomic model of the 70S ribosome from each 3D-EM density map in the previous study [5]. If the model was fitted into the density map, the regions for the bound molecules such as tRNA became apparent (Fig. 1). Based on the shape, the size, and the position with respect to the 70S ribosome of each region, it was determined which bound molecules corresponded to each region. Then, the atomic model was fitted to each region. The same scoring function was used to find the best position and orientation for fitting as in the previous study [5]. For tRNA, the deformed atomic model library was built, which consisted of a lot of deformed atomic models, and the best-fitting one was selected for each region. The deformation of the atomic model was performed by combining the three lowest-frequency normal modes [5], which were obtained from the elastic network model built from all atoms in the X-ray crystal structure (PDB (Protein Data Bank) ID: 3CW5 [6]). In the fitting of the bound molecules, the atomic collision was considered. That is, the fitting calculations were performed in such a way that the atomic model would not collide with the pre-existing best-fitting atomic models. This was achieved by assigning negative density to the regions where the atomic models pre-existed.

Measurement of ratchet angle

First, the 30S and 50S subunits of the X-ray crystal structure of the 70S ribosome [7] was fitted by the RMS-fitting to the corresponding part of the best-fitting atomic model built from each 3D-EM density map and the rotation matrices R_{30} and R_{50} were determined, respectively. By assuming the X-ray crystal structure as the standard conformation, the rotational deformation of the 30S subunit with respect to the 50S subunit is described by the matrix R ($=R_{30}R_{50}^{-1}$). Because any rotational movement of a rigid body can be described by a rotation around a single axis (Euler's rotation theorem), the matrix R can be described by a rotation vector $\boldsymbol{\omega}$ ($=(\omega_x, \omega_y, \omega_z)$), whose direction is the same as the rotation axis and length is the rotation angle. The rotation vector $\boldsymbol{\omega}$ was determined for each of the best-fitting atomic models, and the end point (ω_x, ω_y, ω_z) was plotted in Figure 2. The straight-line $\boldsymbol{l}$ ($=k\boldsymbol{t}+\boldsymbol{p}_0$) in the figure, where $\boldsymbol{t}$ is the unit directional vector and $\boldsymbol{p}_0$ the nearest point on the line to the origin (the dot product of $\boldsymbol{t}$ and $\boldsymbol{p}_0$ is zero; $\boldsymbol{t}\cdot\boldsymbol{p}_0=0$), was drawn in such a way that the sum of the squared distances from all the end points to the line was minimum. The end points were distributed over narrow range around the line, suggesting the existence of a common ratchet axis, which is shown by a yellow arrow in Figure 3. The ratchet angle was defined as the projection of the rotation vector to the line by $\boldsymbol{t}\cdot(\boldsymbol{\omega}-\boldsymbol{p}_0)=\boldsymbol{t}\cdot\boldsymbol{\omega}$, assuming that the ratchet angle for the X-ray crystal structure was zero. Note that there was an ambiguity in the direction of the vector $\boldsymbol{t}$. Thus, the direction of the vector was chosen so that the ratchet angle was positive when the 30S subunit rotated along the direction shown by the cyan arrow in Figure 3.

It should be noted that an internal structural change in each subunit of the best-fitting atomic model from the X-ray crystal structure could affect the ratchet angle, because it could be interpreted partially as the change of the orientation (R_{30} and R_{50}) in the RMS-fitting procedure. The average values of the RMSD from the crystal structure over the best-fitting models analyzed in this study were 2.5 Å and 0.8 Å, respectively, for the 50S and 30S subunits and the maximum values were 4.0 Å and 2.1 Å. The most mobile part in the 50S subunit was the L1 stalk (see Fig. 3), which consisted of less than 5% of the atoms in the subunit, and if this part was ignored in the RMS-fitting, the average and maximum value

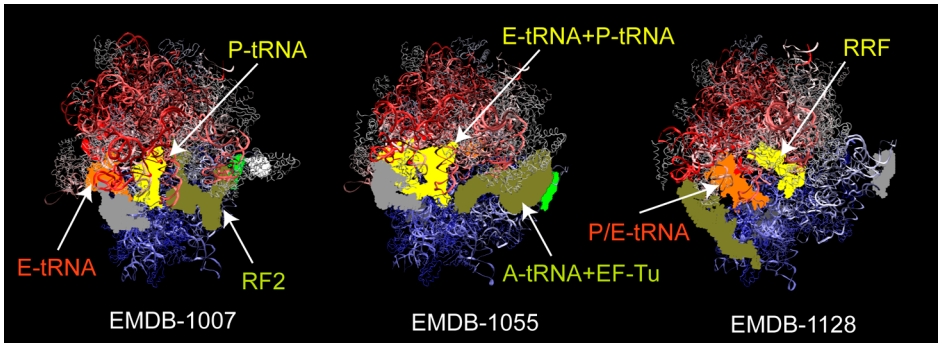

Figure 1 Best-fitting atomic models of the 70S ribosome (ribbon model) fitted into the 3D-EM density maps. In the density map, only the regions that the atomic models did not overlap are painted with colors. The regions with volumes smaller than 8,000 Å^3 are not shown. The EMDB-ID of each density map is shown under each model and map.

of the RMSD for the 50S subunit decreased drastically to 0.9 Å and 1.9 Å, respectively. However, the ratchet angle did not change so much from the original value, and the difference was only 0.25 degree on average and 0.6 degree at a maximum, suggesting that the internal structural change affected little on the ratchet angle. Thus, the RMS-fitting was performed using all atoms in each subunit rather than using the arbitrarily chosen atoms.

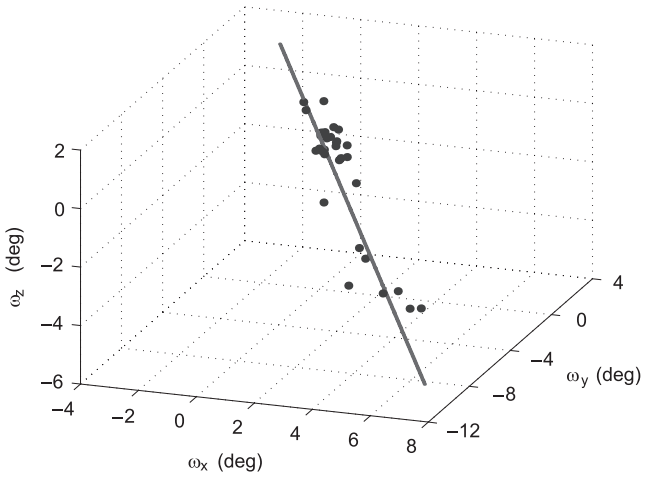

Figure 2 The distribution of the end point of the rotation vector ω. The rotation vector describes the rotational deformation of the 30S subunits with respect to the 50S subunit. See the text for the explanation of the straight line.

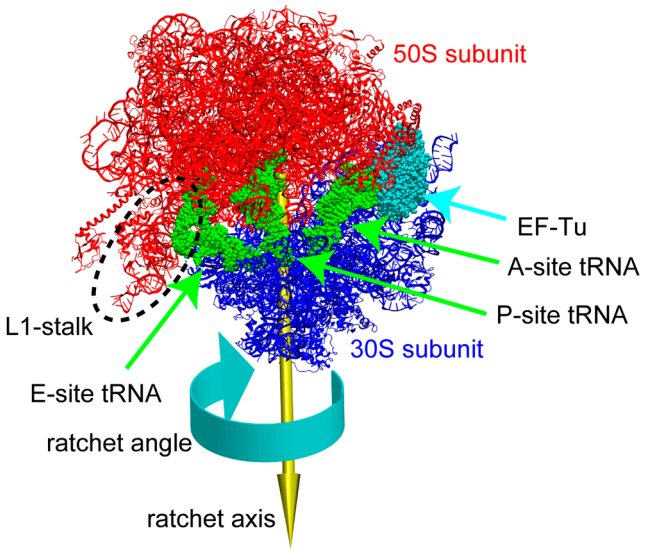

Figure 3 Best-fitting atomic model for a 3D-EM density map (EMDB-5030). The 50S and 30S subunits of the 70S ribosome are painted by red and blue, tRNAs by green and EF-Tu by cyan. The ratchet axis is shown by a yellow arrow.

Results and Discussion

The atomic models were built from the 31 3D-EM density maps of the 70S ribosome, which are listed in Table 1. In the previous study, about 50 density maps[3] were analyzed. Among them, those which were good in the resolution (second column in Table 1) and the clearness of the bound molecules in the density maps, which was checked by the visual inspection, were selected. The X-ray crystal structures with the following PDB ID were used for the model building: 1YL3 [7] and 1YL4 [7] for 70S ribosome, 3CW5 [6] for tRNA, 1B23 [8] for EF-Tu (elongation factor thermo unstable), 2WRI [9] for EF-G (elongation factor G), 3MS0 [10] for RF1 (release factor 1), 2WH1 [11] for RF2 (release factor 2), 2V46 [12] for RRF (ribosome recycling factor). Although the atomic model libraries were built for the 70S ribosome and tRNA, (that is, a lot of deformed atomic models were built for these molecules), those for other bound molecules

Table 1 List of 3D-EM density maps analyzed in this study

EMID	Resolution (Å)[a]	Bound molecule[b]
1003[17][c]	11.5	E, P
1006[18][c]	11.3	E, P
1007[18]	12.9	E, P, RF2
1008[18]	10.9	E, P, RF2
1045[19][c]	16.8	E, P, A, EF-Tu
1055[20][c]	10.25	E, P, A, EF-Tu
1056[20][c]	10.25	E, P, A
1128[21]	14.1	P/E, RRF
1184[22]	12.8	E, P, RF1
1185[22]	14	E, P, RF1
1250[23][c]	15.5	E, P
1261[24]	9.5	P
1262[24]	10.7	P
1263[24]	9.1	P
1310[25][c]	11.8	E, P
1315[26]	7.3	P/E, EF-G
1362[27][c]	12.5	E, P, EF-G
1363[27]	10.9	P/E, EF-G
1365[27]	11.75	P/E, EF-G
1366[27]	12.8	E, P
1370[28]	15.3	P/E, RRF
1395[20][c]	12.8	E, P
1524[29]	10.9	E, P, A, EF4
1540[30][c]	10.5	P, A
1541[30][c]	8.9	P/E, A/P
1564[31][c]	12	E, P, A, EF-Tu
1565[31]	9	P, A, EF-Tu
1798[32]	7.8	P/E, EF-G
1799[32]	7.6	P/E, EF-G
5030[33][c]	6.4	E, P, A, EF-Tu
5036[34][c]	6.7	E, P, A, EF-Tu

[a] The resolutions are based on Fourier shell correlation at 0.5 cut-off.
[b] Only tRNAs and characteristic molecules are shown. E, P, A, P/E, A/P refer to E-site, P-site, A-site, P/E-hybrid site, and A/P-hybrid site tRNAs, respectively.
[c] 3D-EM density maps used for making a movie.

were not built, because the X-ray crystal structures of these molecules fitted very well into the 3D-EM density maps without the deformation.

In Figure 3, the best-fitting atomic model for a 3D-EM density map (EMDB-5030) is shown as an example. In this figure, the ratchet axis is also shown. A ratchet-like global conformational change of the ribosome is known to be important for translocation of tRNA [13]. It is a twisting motion of the 30S subunit with respect to the 50S subunit. By statistically analyzing the 31 best-fitting atomic models of the 70S ribosome, the direction of the common ratchet axis was determined and the ratchet angle was calculated for each atomic model (see methods).

Figure 4 shows the ratchet angle of each best-fitting atomic model of the 70S ribosome. All models have positive ratchet angles. It is clearly seen that the ratchet angle is greatly dependent on the numbers and the sites of the loaded tRNAs. For example, the distribution of the ratchet angles is narrower in the structures loaded with E (exit)-, P (peptidyl)-, and A (aminoacyl)-site tRNAs (including the A-site tRNA bound to EF-Tu, which is often referred to as the A/T-site tRNA) than those loaded with only E- and P-site tRNAs. Also, the distribution is quite large for the structures with P/E hybrid tRNA, which binds to the 30S subunit of the ribosome at the P-site and to the 50S subunit at the E-site. (On the other hand, A/P hybrid tRNA binds to the 30S subunit at the A-site and to the 50S subunit at the P-site.)

From the 14 best-fitting atomic models, we created a movie (Supplementary Movie S1), which shows the conformational changes of the 70S ribosome during the elongation cycle. Each frame of the movie corresponded to the best-fitting atomic model built from a 3D-EM density map. The position and orientation of each model was determined so that the 50S subunit of each model fitted to that of the reference model (RMS-fitting). The sequential order of the frames, or the order in which the best-fitting atomic models appeared in the movie, was determined primarily based on the molecules bound to the ribosome. That is, the ribosome was assumed to be bound to the molecules in the following order (see Fig. 5); (a) E-, P-, A-site tRNAs and EF-Tu, (b) E-, P-, and A-site tRNAs, (c) P- and A-site tRNAs, (d) P/E and A/P-hybrid tRNAs, (e) E- and P-tRNAs and EF-G, (f) E- and P-tRNAs, and went back to (a). There were multiple density maps for the states (a) and (f). For the models in these states, the order was determined based on the values of the ratchet angles so that the ribosome changed its conformation smoothly in the movie. To be precise, it was determined so that the total sum of the absolute value of the change of the ratchet angle during the cycle became minimum. This problem was similar to the "traveling salesman problem".

The movie revealed several interesting points. One is that the variations of the positions and conformations of the A- and P-site tRNAs were small, although the EM density maps were determined by several different groups and the resolutions were different. Especially, the positions of the A-site

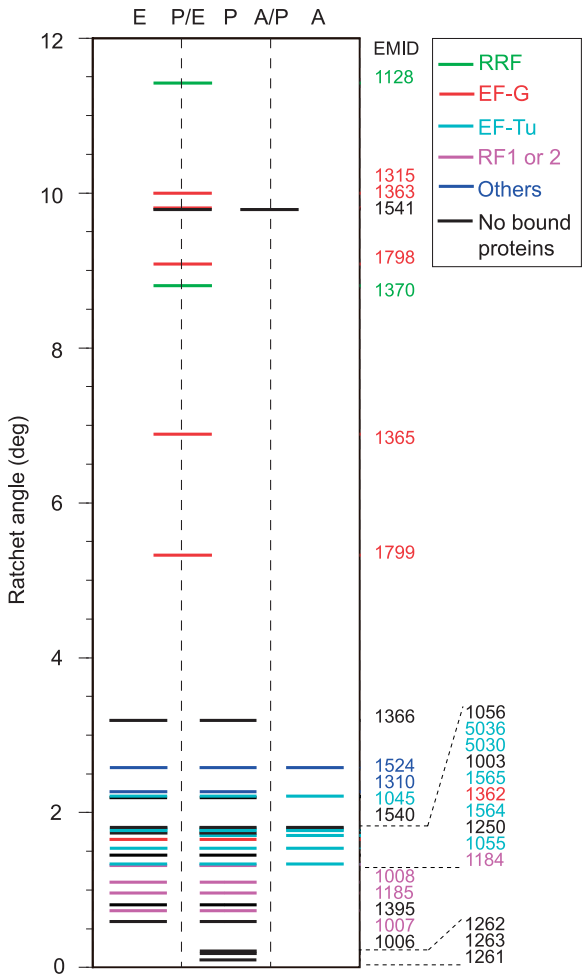

Figure 4 Distribution of ratchet angles of the 70S ribosome. The ratchet angle is indicated by the vertical position of the bar. The sites in which tRNAs reside and the names of the bound proteins are also indicated respectively by the horizontal position and the color of the bar.

tRNA bound with EF-Tu varied little with respect to the 30S subunit (data not shown). The atomic models were built from the six different 3D-EM density maps with EF-Tu/A-tRNA complex (Table 1), in which there were three different types of A-tRNAs, that is, tRNAs for different amino acids. Yet, the variations of the positions of the tRNAs were small. Perhaps, larger contact area with the ribosome by the EF-Tu/A-tRNA complex than the tRNA alone (1880 Å^2 versus 1170 Å^2, which were measured as the decrease of the solvent-accessible surface area (SASA) of the X-ray crystal structure of the 70S ribosome (PDB ID: 2WRN and 2WRO [14]) by the bound molecules) contributed to the small variations, which should be important for the precise translation of the mRNA. In contrast, those for the E-site tRNA were large. This was probably because the density for the E-site tRNA was generally low. The tRNA exits from the E-site, and if it happens, the site becomes empty, which would bring about the low density. Another point is that the L1-stalk (see Fig. 3) seemed to aid the move-

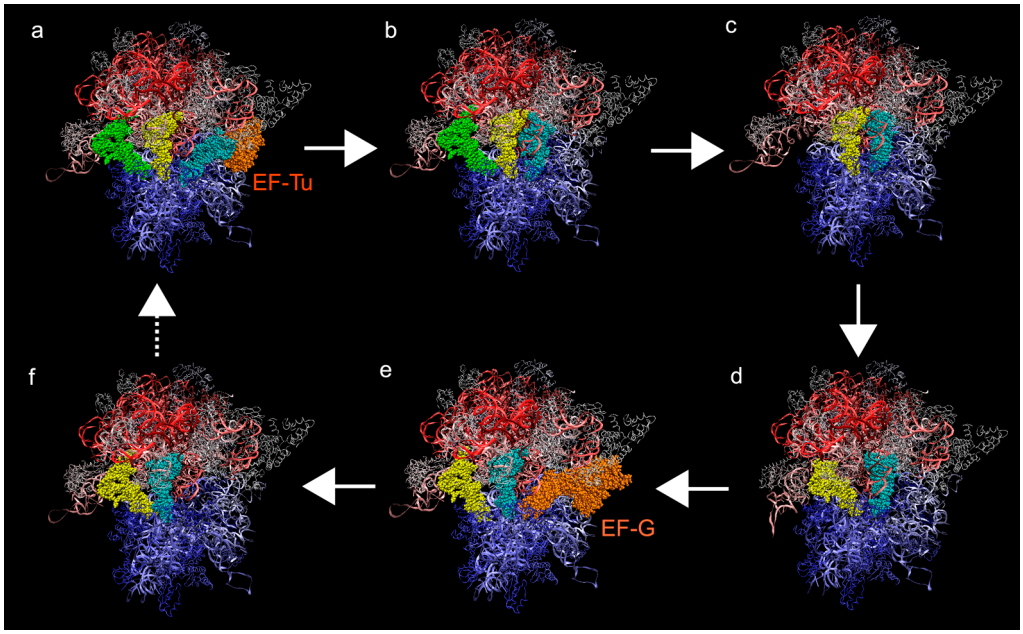

Figure 5 Elongation cycle of the 70S ribosome represented by the best-fitting atomic models. The atomic models were built from the following 3D-EM density maps; (a) EMDB-5030, (b) EMDB-1056, (c) EMDB-1540, (d) EMDB-1541, (e) EMDB-1362, and (f) EMDB-1366. Supplementary Movie S1 online gives more detailed views.

ment of the P/E-site tRNA to the E-site. This is consistent with the single-molecule FRET experiment [15], which suggested that the L1 stalk acted to direct tRNA movements during translocation. The other point is that the large bending deformation was observed at the anticodon stem region of the tRNAs, which was close to the 30S subunit, when the tRNAs moved to the adjacent site, suggesting the importance of the flexibility of the tRNA for the translocation.

Conclusion

In this study, the atomic models of the 70S ribosome, including the bound molecules, were built from the 3D-EM density maps and a movie for the elongation cycle was made using the resultant models. Recent development of the cryo-electron microscopy sometimes enables structural analysis of macromolecules nearly at the atomic resolution. In such cases, conventional modeling approaches, such as those used in the X-ray crystallography, could be applicable and the detailed structural analysis would be possible. In this study, the density maps with relatively low resolution (from the point of view of the present electron microscopy) were used. Thus, the global conformational differences between the models were the main targets, because the accuracy of the details of the models might not be so high. Still, the movie revealed several interesting points which were not apparent from each density map, suggesting the usefulness of a movie made from many 3D-EM density maps. It may inspire researchers to design new biological experiments (or computer simulations) and promote a further understanding of the macromolecules as a result.

In making a movie, one of the important tasks is to determine the sequential order in which the atomic models appear in the movie. The order must reflect the conformational changes in the biological environment. However, it cannot be determined from the 3D-EM density maps. Other experimental results are necessary. In this study, the knowledge about the bound molecules and the values of the ratchet angle were used. As to the ratchet angle, a new way for measuring the ratchet angle was developed, in which the ratchet axis was determined statistically.

Acknowledgments

Molecular graphics were performed using the software VMD [16]. This work was supported by grants from the Platform Project for Supporting in Drug Discovery and Life Science Research (Platform for Drug Discovery, Informatics, and Structural Life Science) from Japan Agency for Medical Research and Development (AMED), and JSPS KAKENHI Grant Numbers JP18K06101.

Conflicts of Interest

The author declares no conflicts of interest.

Author Contribution

The author directed the research and wrote the manuscript

References

[1] Frank, J. Three-Dimensional Reconstruction. in *Three-Dimensional Electron Microscopy of Macromolecular Assemblies*. pp. 182–246 (Academic Press, Burlington, 1996).

[2] Tama, F., Miyashita, O. & Brooks, C. L., 3rd. Normal mode based flexible fitting of high-resolution structure into low-resolution experimental data from cryo-EM. *J. Struct. Biol.* **147**, 315–326 (2004).

[3] Tama, F., Miyashita, O. & Brooks, C. L., 3rd. Flexible multi-scale fitting of atomic structures into low-resolution electron density maps with elastic network normal mode analysis. *J. Mol. Biol.* **337**, 985–999 (2004).

[4] Trabuco, L. G., Villa, E., Mitra, K., Frank, J. & Schulten, K. Flexible fitting of atomic structures into electron microscopy maps using molecular dynamics. *Structure* **16**, 673–683 (2008).

[5] Matsumoto, A. & Ishida, H. Global conformational changes of ribosome observed by normal mode fitting for 3D Cryo-EM structures. *Structure* **17**, 1605–1613 (2009).

[6] Barraud, P., Schmitt, E., Mechulam, Y., Dardel, F. & Tisne, C. A unique conformation of the anticodon stem-loop is associated with the capacity of tRNAfMet to initiate protein synthesis. *Nucleic Acids Res.* **36**, 4894–4901 (2008).

[7] Jenner, L., Romby, P., Rees, B., Schulze-Briese, C., Springer, M., Ehresmann, C., *et al.* Translational operator of mRNA on the ribosome: how repressor proteins exclude ribosome binding. *Science* **308**, 120–123 (2005).

[8] Nissen, P., Thirup, S., Kjeldgaard, M. & Nyborg, J. The crystal structure of Cys-tRNACys-EF-Tu-GDPNP reveals general and specific features in the ternary complex and in tRNA. *Structure* **7**, 143–156 (1999).

[9] Gao, Y. G., Selmer, M., Dunham, C. M., Weixlbaumer, A., Kelley, A. C. & Ramakrishnan, V. The structure of the ribosome with elongation factor G trapped in the posttranslocational state. *Science* **326**, 694–699 (2009).

[10] Korostelev, A., Zhu, J., Asahara, H. & Noller, H. F. Recognition of the amber UAG stop codon by release factor RF1. *EMBO J.* **29**, 2577–2585 (2010).

[11] Weixlbaumer, A., Jin, H., Neubauer, C., Voorhees, R. M., Petry, S., Kelley, A. C., *et al.* Insights into translational termination from the structure of RF2 bound to the ribosome. *Science* **322**, 953–956 (2008).

[12] Weixlbaumer, A., Petry, S., Dunham, C. M., Selmer, M., Kelley, A. C. & Ramakrishnan, V. Crystal structure of the ribosome recycling factor bound to the ribosome. *Nat. Struct. Mol. Biol.* **14**, 733–737 (2007).

[13] Frank, J. & Agrawal, R. K. A ratchet-like inter-subunit reorganization of the ribosome during translocation. *Nature* **406**, 318–322 (2000).

[14] Schmeing, T. M., Voorhees, R. M., Kelley, A. C., Gao, Y. G., Murphy, F. V., 4th., Weir, J. R., *et al.* The crystal structure of the ribosome bound to EF-Tu and aminoacyl-tRNA. *Science* **326**, 688–694 (2009).

[15] Fei, J., Kosuri, P., MacDougall, D. D. & Gonzalez, R. L. Coupling of Ribosomal L1 Stalk and tRNA Dynamics during Translation Elongation. *Mol. Cell* **30**, 348–359 (2008).

[16] Humphrey, W., Dalke, A. & Schulten, K. VMD: visual molecular dynamics. *J. Mol. Graph.* **14**, 33–38, 27–38 (1996).

[17] Gabashvili, I. S., Agrawal, R. K., Spahn, C. M., Grassucci, R. A., Svergun, D. I., Frank, J., *et al.* Solution structure of the E. coli 70S ribosome at 11.5 A resolution. *Cell* **100**, 537–549 (2000).

[18] Rawat, U. B., Zavialov, A. V., Sengupta, J., Valle, M., Grassucci, R. A., Linde, J., *et al.* A cryo-electron microscopic study of ribosome-bound termination factor RF2. *Nature* **421**, 87–90 (2003).

[19] Valle, M., Sengupta, J., Swami, N. K., Grassucci, R. A., Burkhardt, N., Nierhaus, K. H., *et al.* Cryo-EM reveals an active role for aminoacyl-tRNA in the accommodation process. *EMBO J.* **21**, 3557–3567 (2002).

[20] Valle, M., Zavialov, A., Li, W., Stagg, S. M., Sengupta, J., Nielsen, R. C., *et al.* Incorporation of aminoacyl-tRNA into the ribosome as seen by cryo-electron microscopy. *Nat. Struct. Biol.* **10**, 899–906 (2003).

[21] Gao, N., Zavialov, A. V., Li, W., Sengupta, J., Valle, M., Gursky, R. P., *et al.* Mechanism for the disassembly of the posttermination complex inferred from cryo-EM studies. *Mol. Cell* **18**, 663–674 (2005).

[22] Rawat, U., Gao, H., Zavialov, A., Gursky, R., Ehrenberg, M. & Frank, J. Interactions of the release factor RF1 with the ribosome as revealed by cryo-EM. *J. Mol. Biol.* **357**, 1144–1153 (2006).

[23] Schaffitzel, C., Oswald, M., Berger, I., Ishikawa, T., Abrahams, J. P., Koerten, H. K., *et al.* Structure of the E. coli signal recognition particle bound to a translating ribosome. *Nature* **444**, 503–506 (2006).

[24] Halic, M., Blau, M., Becker, T., Mielke, T., Pool, M. R., Wild, K., *et al.* Following the signal sequence from ribosomal tunnel exit to signal recognition particle. *Nature* **444**, 507–511 (2006).

[25] Gillet, R., Kaur, S., Li, W., Hallier, M., Felden, B. & Frank, J. Scaffolding as an organizing principle in trans-translation. The roles of small protein B and ribosomal protein S1. *J. Biol. Chem.* **282**, 6356–6363 (2007).

[26] Connell, S. R., Takemoto, C., Wilson, D. N., Wang, H., Murayama, K., Terada, T., *et al.* Structural basis for interaction of the ribosome with the switch regions of GTP-bound elongation factors. *Mol. Cell* **25**, 751–764 (2007).

[27] Valle, M., Zavialov, A., Sengupta, J., Rawat, U., Ehrenberg, M. & Frank, J. Locking and unlocking of ribosomal motions. *Cell* **114**, 123–134 (2003).

[28] Barat, C., Datta, P. P., Raj, V. S., Sharma, M. R., Kaji, H., Kaji, A., *et al.* Progression of the ribosome recycling factor through the ribosome dissociates the two ribosomal subunits. *Mol. Cell* **27**, 250–261 (2007).

[29] Connell, S. R., Topf, M., Qin, Y., Wilson, D. N., Mielke, T., Fucini, P., *et al.* A new tRNA intermediate revealed on the ribosome during EF4-mediated back-translocation. *Nat. Struct. Mol. Biol.* **15**, 910–915 (2008).

[30] Agirrezabala, X., Lei, J., Brunelle, J. L., Ortiz-Meoz, R. F., Green, R. & Frank, J. Visualization of the hybrid state of tRNA binding promoted by spontaneous ratcheting of the ribosome. *Mol. Cell* **32**, 190–197 (2008).

[31] Li, W., Agirrezabala, X., Lei, J., Bouakaz, L., Brunelle, J. L., Ortiz-Meoz, R. F., *et al.* Recognition of aminoacyl-tRNA: a common molecular mechanism revealed by cryo-EM. *EMBO J.* **27**, 3322–3331 (2008).

[32] Ratje, A. H., Loerke, J., Mikolajka, A., Brunner, M., Hildebrand, P. W., Starosta, A. L., *et al.* Head swivel on the ribosome facilitates translocation by means of intra-subunit tRNA hybrid sites. *Nature* **468**, 713–716.

[33] Schuette, J. C., Murphy, F. V., 4th., Kelley, A. C., Weir, J. R., Giesebrecht, J., Connell, S. R., *et al.* GTPase activation of elongation factor EF-Tu by the ribosome during decoding. *EMBO J.* **28**, 755–765 (2009).

[34] Villa, E., Sengupta, J., Trabuco, L. G., LeBarron, J., Baxter, W. T., Shaikh, T. R., *et al.* Ribosome-induced changes in elongation factor Tu conformation control GTP hydrolysis. *Proc. Natl. Acad. Sci. USA* **106**, 1063–1068 (2009).